



## Synthesis of $\text{NaLa}(\text{MoO}_4)_2:\text{Eu}^{3+}/\text{Yb}^{3+}$ Phosphors *via* Microwave-Modified Sol-Gel Route and Their Upconversion Photoluminescence Properties

CHANG SUNG LIM

Department of Advanced Materials Science and Engineering, Hanseo University, Seosan 356-706, Republic of Korea

Corresponding author: Tel/Fax: +82 41 6601445; E-mail: cslim@hanseo.ac.kr

Received: 7 August 2014;

Accepted: 20 November 2014;

Published online: 26 May 2015;

AJC-17242

$\text{NaLa}_{1-x}(\text{MoO}_4)_2:\text{Eu}^{3+}/\text{Yb}^{3+}$  phosphors with doping concentrations of  $\text{Eu}^{3+}$  and  $\text{Yb}^{3+}$  ( $x = \text{Eu}^{3+} + \text{Yb}^{3+}$ ,  $\text{Eu}^{3+} = 0.05, 0.1, 0.2$  and  $\text{Yb}^{3+} = 0.2, 0.45$ ) were successfully synthesized *via* the microwave-modified sol-gel route and the upconversion and spectroscopic properties were investigated. Well-crystallized particles showed a fine and homogeneous morphology with particle sizes of 5-10  $\mu\text{m}$ . Under excitation at 980 nm,  $\text{NaLa}_{0.5}(\text{MoO}_4)_2:\text{Er}_{0.05}\text{Yb}_{0.45}$  particles exhibited a strong 525 nm emission band and a weak 550 nm emission band in the blue region and a very weak 655 nm emission band in the red region. The Raman spectra of  $\text{NaLa}_{0.8}(\text{MoO}_4)_2:\text{Eu}_{0.2}$ ,  $\text{NaLa}_{0.7}(\text{MoO}_4)_2:\text{Eu}_{0.1}\text{Yb}_{0.2}$  and  $\text{NaLa}_{0.5}(\text{MoO}_4)_2:\text{Eu}_{0.05}\text{Yb}_{0.45}$  particles indicated the domination of strong peaks at higher frequencies (762, 890, 1358 and 1430  $\text{cm}^{-1}$ ) and weak peaks at lower frequencies (323, 388 and 450  $\text{cm}^{-1}$ ).

**Keywords:** Phosphors, Microwave sol-gel, Upconversion, Raman spectroscopy.

### INTRODUCTION

The photoluminescence particles have evolved in their applications, such as fluorescent lamps, cathode ray tubes, solid-state laser, amplifiers for fiber optics communication and new optoelectronic devices, which show high luminescence quantum yields, since usually more than one metastable excited state exists, multiple emissions are observed<sup>1,2</sup>. Rare-earth activated upconversion (UC) particles can convert near infrared radiation of low energy into visible radiation of high energy. Recently, the synthesis and the luminescence properties of upconversion particles have attracted considerable interest since they are considered as potentially active components in new optoelectronic devices and luminescent labels for imaging and biodetection assays, which overcome the current limitations in traditional photoluminescence materials<sup>3</sup>. The double molybdate compounds of  $\text{MR}_2(\text{MoO}_4)_4$  (M: bivalent alkaline earth metal ion, R: trivalent rare earth ion) belong to a group of double alkaline earth lanthanide molybdates. With the decrease in the ionic radius of alkaline earth metal ions, it is possible for the structure of  $\text{MR}_2(\text{MoO}_4)_4$  to be transformed to a highly disordered tetragonal Scheelite structure from the monoclinic structure. It is possible for the trivalent rare earth ions in the disordered tetragonal-phase to be partially substituted by  $\text{Eu}^{3+}$  and  $\text{Yb}^{3+}$  ions, these ions are effectively doped into the crystal lattices of the tetragonal phase due to the similar radii of the trivalent rare-earth ions ( $\text{Re}^{3+}$ ). This results in the

excellent upconversion photoluminescence properties<sup>4-6</sup>. Among rare-earth ions, the  $\text{Eu}^{3+}$  ion is suitable for converting infrared to visible light through the upconversion process due to its appropriate electronic energy level configuration. The co-doped  $\text{Yb}^{3+}$  ion and  $\text{Eu}^{3+}$  ion can remarkably enhance the upconversion efficiency for the shift from infrared to visible light due to the efficiency of the energy transfer from  $\text{Yb}^{3+}$  to  $\text{Eu}^{3+}$ . The  $\text{Yb}^{3+}$  ion, as a sensitizer, can be effectively excited by an incident light source energy. This energy is transferred to the activator from which radiation can be emitted<sup>7-9</sup>.

Rare-earth activated double molybdates has attracted great attention because of its spectroscopic characteristics and excellent upconversion photoluminescence properties. Several processes have been developed to prepare these rare-earth doped double molybdates. Usually, the sol-gel process provides some advantages over the conventional solid-state method, including good homogeneity, low calcination temperature, small particle size and narrow particle size distribution optimal for good luminescent characteristics. However, the sol-gel process has a disadvantage in that it takes a long time for gelation. Compared with the usual methods, microwave synthesis has the advantages of a very short reaction time, small-size particles, narrow particle size distribution and high purity of final polycrystalline samples. Microwave heating is delivered to the material surface by radiant and/or convection heating, which is transferred to the bulk of the material *via* conduction<sup>10,11</sup>. A microwave-modified sol-gel route is a cost-effective

method that provides high homogeneity and is easy to scale-up and it is emerging as a viable alternative approach for the quick synthesis of high-quality luminescent materials.

In this study,  $\text{NaLa}_{1-x}(\text{MoO}_4)_2:\text{Eu}^{3+}/\text{Yb}^{3+}$  phosphors with doping concentrations of  $\text{Eu}^{3+}$  and  $\text{Yb}^{3+}$  ( $x = \text{Eu}^{3+} + \text{Yb}^{3+}$ ,  $\text{Eu}^{3+} = 0.05, 0.1, 0.2$  and  $\text{Yb}^{3+} = 0.2, 0.45$ ) phosphors were prepared *via* the microwave-modified sol-gel route followed by heat treatment. The synthesized particles were characterized by X-ray diffraction (XRD), scanning electron microscopy (SEM) and energy-dispersive X-ray spectroscopy (EDS). The optical properties were examined comparatively using photoluminescence (PL) emission and Raman spectroscopy.

## EXPERIMENTAL

Appropriate stoichiometric amounts of  $\text{Na}_2\text{MoO}_4 \cdot 2\text{H}_2\text{O}$  (99 %, Sigma-Aldrich, USA),  $\text{La}(\text{NO}_3)_3 \cdot 6\text{H}_2\text{O}$  (99 %, Sigma-Aldrich, USA),  $(\text{NH}_4)_6\text{Mo}_7\text{O}_{24} \cdot 4\text{H}_2\text{O}$  (99 %, Alfa Aesar, USA),  $\text{Eu}(\text{NO}_3)_3 \cdot 5\text{H}_2\text{O}$  (99.9 %, Sigma-Aldrich, USA),  $\text{Yb}(\text{NO}_3)_3 \cdot 5\text{H}_2\text{O}$  (99.9 %, Sigma-Aldrich, USA), citric acid (99.5 %, Daejung Chemicals, Korea),  $\text{NH}_4\text{OH}$  (A.R.), ethylene glycol (A.R.) and distilled water were used to prepare  $\text{NaLa}(\text{MoO}_4)_2$ ,  $\text{NaLa}_{0.8}(\text{MoO}_4)_2:\text{Eu}_{0.2}$ ,  $\text{NaLa}_{0.7}(\text{MoO}_4)_2:\text{Eu}_{0.1}\text{Yb}_{0.2}$  and  $\text{NaLa}_{0.5}(\text{MoO}_4)_2:\text{Eu}_{0.05}\text{Yb}_{0.45}$  compounds with doping concentrations of  $\text{Eu}^{3+}$  and  $\text{Yb}^{3+}$  ( $\text{Eu}^{3+} = 0.05, 0.1, 0.2$  and  $\text{Yb}^{3+} = 0.2, 0.45$ ). To prepare  $\text{NaLa}(\text{MoO}_4)_2$ , 0.2 mol %  $\text{Na}_2\text{MoO}_4 \cdot 2\text{H}_2\text{O}$  and 0.114 mol %  $(\text{NH}_4)_6\text{Mo}_7\text{O}_{24} \cdot 4\text{H}_2\text{O}$  were dissolved in 20 mL of ethylene glycol and 80 mL of 5 M  $\text{NH}_4\text{OH}$  under vigorous stirring and heating. Subsequently, 0.4 mol %  $\text{La}(\text{NO}_3)_3 \cdot 6\text{H}_2\text{O}$  and citric acid (with a molar ratio of citric acid to total metal ions of 2:1) were dissolved in 100 mL of distilled water under vigorous stirring and heating. Then, the solutions were mixed together under vigorous stirring and heating at 80-100 °C. At the end, highly transparent solutions were obtained and adjusted to pH = 7-8 by the addition of  $\text{NH}_4\text{OH}$  or citric acid. In order to prepare  $\text{NaLa}_{0.8}(\text{MoO}_4)_2:\text{Er}_{0.2}$ , the mixture of 0.32 mol %  $\text{La}(\text{NO}_3)_3 \cdot 6\text{H}_2\text{O}$  with 0.08 mol %  $\text{Eu}(\text{NO}_3)_3 \cdot 5\text{H}_2\text{O}$  was used for the creation of the rare earth solution. In order to prepare  $\text{NaLa}_{0.7}(\text{MoO}_4)_2:\text{Eu}_{0.1}\text{Yb}_{0.2}$ , the mixture of 0.28 mol %  $\text{La}(\text{NO}_3)_3 \cdot 6\text{H}_2\text{O}$  with 0.04 mol %  $\text{Eu}(\text{NO}_3)_3 \cdot 5\text{H}_2\text{O}$  and 0.08 mol %  $\text{Yb}(\text{NO}_3)_3 \cdot 5\text{H}_2\text{O}$  was used for the creation of the rare earth solution. In order to prepare  $\text{NaLa}_{0.5}(\text{MoO}_4)_2:\text{Eu}_{0.05}\text{Yb}_{0.45}$ , the rare earth containing solution was generated using 0.2 mol %  $\text{La}(\text{NO}_3)_3 \cdot 6\text{H}_2\text{O}$  with 0.02 mol %  $\text{Eu}(\text{NO}_3)_3 \cdot 5\text{H}_2\text{O}$  and 0.18 mol %  $\text{Yb}(\text{NO}_3)_3 \cdot 5\text{H}_2\text{O}$ .

The transparent solutions were placed into a microwave oven operating at a frequency of 2.45 GHz with a maximum output-power of 1250 W for 0.5 h. The working cycle of the microwave reaction was controlled precisely using a regime of 40 s on and 20 s off for 15 min, followed by further treatment of 30 s on and 30 s off for 15 min. The samples were treated with ultrasonic radiation for 10 min to produce a light yellow transparent sol. After this, the light yellow transparent sols were dried at 120 °C in a dry oven to obtain black dried gels. The black dried gels were grinded and heat-treated at 900 °C for 16 h with 100 °C intervals between 600-900 °C. Finally, white particles were obtained for  $\text{NaLa}(\text{MoO}_4)_2$  and pink particles for the doped compositions.

The phase composition of the synthesized particles was identified using XRD (D/MAX 2200, Rigaku, Japan). The

microstructure and surface morphology of the  $\text{NaLa}(\text{MoO}_4)_2$ ,  $\text{NaLa}_{0.8}(\text{MoO}_4)_2:\text{Eu}_{0.2}$ ,  $\text{NaLa}_{0.7}(\text{MoO}_4)_2:\text{Eu}_{0.1}\text{Yb}_{0.2}$  and  $\text{NaLa}_{0.5}(\text{MoO}_4)_2:\text{Eu}_{0.05}\text{Yb}_{0.45}$  particles were observed using SEM/EDS (JSM-5600, JEOL, Japan). The PL spectra were recorded using a spectrophotometer (Perkin Elmer LS55, UK) at room temperature. Raman spectroscopy measurements were performed using a LabRam Aramis (Horiba Jobin-Yvon, France). The 514.5 nm line of an Ar ion laser was used as the excitation source and the power on the samples was kept at 0.5 mW.

## RESULTS AND DISCUSSION

Fig. 1 shows the X-ray diffraction patterns of the (a) JCPDS 24-1103 data of  $\text{NaLa}(\text{MoO}_4)_2$ , the synthesized (b)  $\text{NaLa}(\text{MoO}_4)_2$ , (c)  $\text{NaLa}_{0.8}(\text{MoO}_4)_2:\text{Eu}_{0.2}$ , (d)  $\text{NaLa}_{0.7}(\text{MoO}_4)_2:\text{Eu}_{0.1}\text{Yb}_{0.2}$  and (e)  $\text{NaLa}_{0.5}(\text{MoO}_4)_2:\text{Eu}_{0.05}\text{Yb}_{0.45}$  particles. The diffraction patterns of the products can be mostly consistent with the standard data of  $\text{NaLa}(\text{MoO}_4)_2$  (JCPDS 24-1103). No impurity phases were detected.  $\text{NaLa}(\text{MoO}_4)_2$  as a member of double molybdate family has a Scheelite structure with the lattice constants of  $a = 5.345 \text{ \AA}$  and  $c = 11.790 \text{ \AA}$ <sup>12</sup>. Which is tetragonal with space group  $I4_{1/a}$ . In  $\text{NaLa}(\text{MoO}_4)_2$  matrix,  $\text{Na}^+$  and  $\text{La}^{3+}$  are randomly arranged and form a disordered structure.  $\text{Eu}^{3+}$  and  $\text{Yb}^{3+}$  ions can be effectively doped in the  $\text{NaLa}(\text{MoO}_4)_2$  lattice by partial substitution of  $\text{La}^{3+}$  site due to the similar radii of  $\text{La}^{3+}$  and by  $\text{Eu}^{3+}$  and  $\text{Yb}^{3+}$ . Post heat-treatment plays an important role in a well-defined crystallized morphology. To achieve a well-defined crystalline morphology,  $\text{NaLa}(\text{MoO}_4)_2$ ,  $\text{NaLa}_{0.8}(\text{MoO}_4)_2:\text{Eu}_{0.2}$ ,  $\text{NaLa}_{0.7}(\text{MoO}_4)_2:\text{Eu}_{0.1}\text{Yb}_{0.2}$  and  $\text{NaLa}_{0.5}(\text{MoO}_4)_2:\text{Eu}_{0.05}\text{Yb}_{0.45}$  phases need to be heat treated at 900 °C for 16 h. It is assumed that the doping amount of  $\text{Eu}^{3+}/\text{Yb}^{3+}$  has a great effect on the crystalline cell volume of the  $\text{NaLa}(\text{MoO}_4)_2$ , because of the different ionic sizes and energy band gaps.

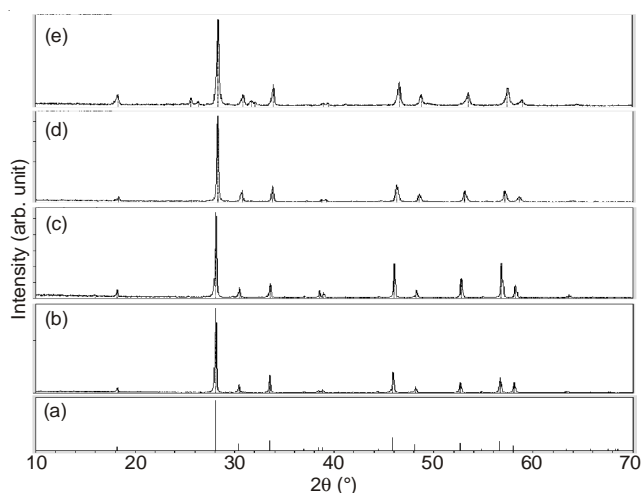


Fig. 1. X-ray diffraction patterns of the (a) JCPDS 24-1103 data of  $\text{NaLa}(\text{MoO}_4)_2$ , the synthesized (b)  $\text{NaLa}(\text{MoO}_4)_2$ , (c)  $\text{NaLa}_{0.8}(\text{MoO}_4)_2:\text{Eu}_{0.2}$ , (d)  $\text{NaLa}_{0.7}(\text{MoO}_4)_2:\text{Eu}_{0.1}\text{Yb}_{0.2}$ , and (e)  $\text{NaLa}_{0.5}(\text{MoO}_4)_2:\text{Eu}_{0.05}\text{Yb}_{0.45}$  particles

Fig. 2 shows a SEM image of the synthesized  $\text{NaLa}_{0.5}(\text{MoO}_4)_2:\text{Eu}_{0.05}\text{Yb}_{0.45}$  particles. The as-synthesized samples are well crystallized with a fine and homogeneous morphology and particle size of 5-10  $\mu\text{m}$ . It is noted that the obtained sample

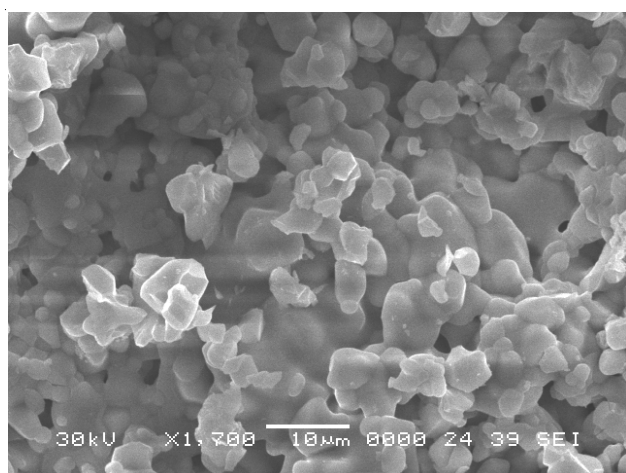


Fig. 2. Scanning electron microscopy image of the synthesized  $\text{NaLa}_{0.5}(\text{MoO}_4)_2:\text{Eu}_{0.05}\text{Yb}_{0.45}$  particles

possesses a partial substitution of  $\text{La}^{3+}$  by  $\text{Eu}^{3+}$  and  $\text{Yb}^{3+}$  ions and the ions are effectively doped into crystal lattices of the  $\text{NaLa}(\text{MoO}_4)_2$  phase due to the similar radii of  $\text{La}^{3+}$ ,  $\text{Eu}^{3+}$  and  $\text{Yb}^{3+}$ . This suggests that the cyclic microwave-modified sol-gel route is suitable for the growth of  $\text{NaLa}_{1-x}(\text{MoO}_4)_2:\text{Eu}^{3+}/\text{Yb}^{3+}$  crystallites.

Fig. 3 shows the energy-dispersive X-ray spectroscopy patterns of the synthesized (a)  $\text{NaLa}_{0.8}(\text{MoO}_4)_2:\text{Eu}_{0.2}$  and (b)  $\text{NaLa}_{0.5}(\text{MoO}_4)_2:\text{Eu}_{0.05}\text{Yb}_{0.45}$  particles and quantitative compositions of (c)  $\text{NaLa}_{0.8}(\text{MoO}_4)_2:\text{Eu}_{0.2}$  and (d)  $\text{NaLa}_{0.5}(\text{MoO}_4)_2:\text{Eu}_{0.05}\text{Yb}_{0.45}$  particles. The EDS pattern shows that the (a)  $\text{NaLa}_{0.8}(\text{MoO}_4)_2:\text{Eu}_{0.2}$  and (b)  $\text{NaLa}_{0.5}(\text{MoO}_4)_2:\text{Eu}_{0.05}\text{Yb}_{0.45}$  particles are composed of Na, La, Mo, O and Eu for  $\text{NaLa}_{0.8}(\text{MoO}_4)_2:\text{Eu}_{0.2}$  and Na, La, Mo, O, Eu and Yb for  $\text{NaLa}_{0.5}(\text{MoO}_4)_2:\text{Eu}_{0.05}\text{Yb}_{0.45}$  particles. The quantitative compositions of (c) and (d) are in good relation with nominal compositions of the particles. The relation of Na, La, Mo, O, Eu and Yb components exhibit that  $\text{NaLa}_{0.8}(\text{MoO}_4)_2:\text{Eu}_{0.2}$  and  $\text{NaLa}_{0.5}(\text{MoO}_4)_2:\text{Eu}_{0.05}\text{Yb}_{0.45}$  particles can be successfully synthesized using the microwave-modified sol-gel method. The microwave-modified sol-gel process of double tungstates provides the energy to synthesize the bulk of the material uniformly, so that fine particles with controlled morphology can be fabricated in a short time period.

Fig. 4 shows the upconversion photoluminescence emission spectra of the as-prepared (a)  $\text{NaLa}(\text{MoO}_4)_2$ , (b)  $\text{NaLa}_{0.8}(\text{MoO}_4)_2:\text{Eu}_{0.2}$ , (c)  $\text{NaLa}_{0.7}(\text{MoO}_4)_2:\text{Eu}_{0.1}\text{Yb}_{0.2}$  and (d)  $\text{NaLa}_{0.5}(\text{MoO}_4)_2:\text{Eu}_{0.05}\text{Yb}_{0.45}$  particles excited under 980 nm at room temperature. The upconversion intensities of (c)  $\text{NaLa}_{0.7}(\text{MoO}_4)_2:\text{Eu}_{0.1}\text{Yb}_{0.2}$  and (d)  $\text{NaLa}_{0.5}(\text{MoO}_4)_2:\text{Eu}_{0.05}\text{Yb}_{0.45}$  particles exhibited a strong 525 nm and a weak 550 nm emission bands and in the green region and a very weak 655 nm emission band in the red region. The strong 525 nm emission and the weak 550 nm in the green region correspond to the  ${}^7\text{F}_1 \rightarrow {}^5\text{D}_1$  transition and  ${}^5\text{D}_1 \rightarrow {}^7\text{F}_1$  transition, respectively. The very weak emission 655 nm band in the red region corresponds to the  ${}^3\text{D}_0 \rightarrow {}^7\text{F}_3$  transition. The upconversion intensities of (a)  $\text{NaLa}(\text{MoO}_4)_2$  were not detected and the upconversion intensities of (b)  $\text{NaLa}_{0.8}(\text{MoO}_4)_2:\text{Eu}_{0.2}$  shows a very weak 525 and 550 nm emission bands and in the green region and a very weak 655 nm emission band in the red region. The upconversion intensity

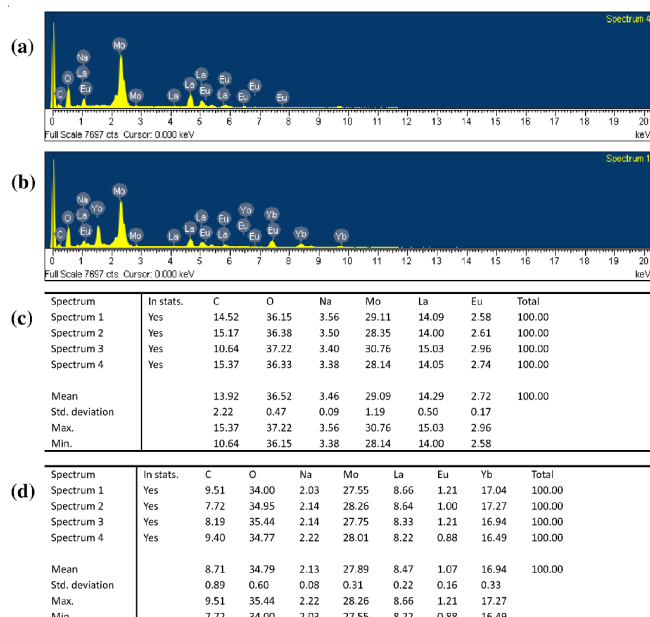


Fig. 3. Energy-dispersive X-ray spectroscopy patterns of the synthesized (a)  $\text{NaLa}_{0.8}(\text{MoO}_4)_2:\text{Eu}_{0.2}$  and (b)  $\text{NaLa}_{0.5}(\text{MoO}_4)_2:\text{Eu}_{0.05}\text{Yb}_{0.45}$  particles, and quantitative compositions of (c)  $\text{NaLa}_{0.8}(\text{MoO}_4)_2:\text{Eu}_{0.2}$  and (d)  $\text{NaLa}_{0.5}(\text{MoO}_4)_2:\text{Eu}_{0.05}\text{Yb}_{0.45}$  particles

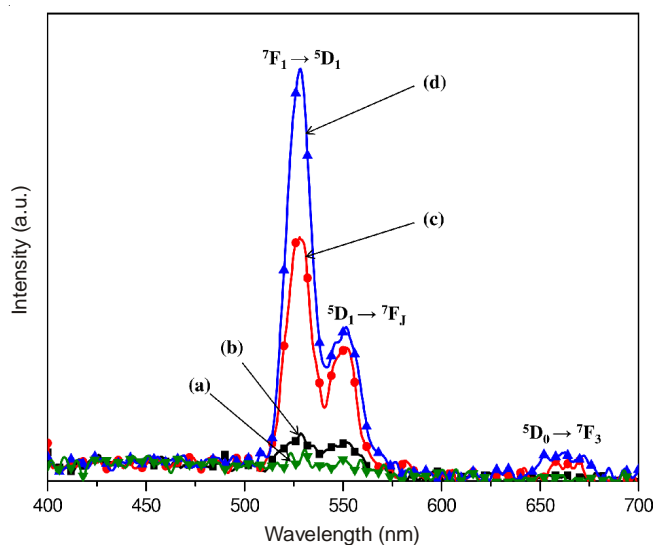


Fig. 4. Upconversion photoluminescence emission spectra of (a)  $\text{NaLa}(\text{MoO}_4)_2$ , (b)  $\text{NaLa}_{0.8}(\text{MoO}_4)_2:\text{Eu}_{0.2}$ , (c)  $\text{NaLa}_{0.7}(\text{MoO}_4)_2:\text{Eu}_{0.1}\text{Yb}_{0.2}$  and (d)  $\text{NaLa}_{0.5}(\text{MoO}_4)_2:\text{Eu}_{0.05}\text{Yb}_{0.45}$  particles excited under 980 nm at room temperature

intensity of (d)  $\text{NaLa}_{0.5}(\text{MoO}_4)_2:\text{Eu}_{0.05}\text{Yb}_{0.45}$  is much higher than that of (c)  $\text{NaLa}_{0.7}(\text{MoO}_4)_2:\text{Eu}_{0.1}\text{Yb}_{0.2}$  particles. The doping amounts of  $\text{Eu}^{3+}/\text{Yb}^{3+}$  had a great effect on the morphological features of the particles and their upconversion fluorescence intensity. The  $\text{Yb}^{3+}$  ion sensitizer can be effectively excited by the energy of an incident light source, this energy is transferred to the activator where radiation can be emitted. The  $\text{Eu}^{3+}$  ion activator is the luminescence center for these upconversion particles and the sensitizer  $\text{Yb}^{3+}$  enhances the upconversion luminescence efficiency<sup>13,14</sup>.

Fig. 5 shows the Raman spectra of the synthesized Raman spectra of the synthesized (a)  $\text{NaLa}(\text{MoO}_4)_2(\text{NLM})$ , (b)  $\text{NaLa}_{0.5}(\text{MoO}_4)_2:\text{Eu}_{0.05}\text{Yb}_{0.45}(\text{NLM}:\text{Eu})$ , (c)  $\text{NaLa}_{0.7}(\text{MoO}_4)_2:$

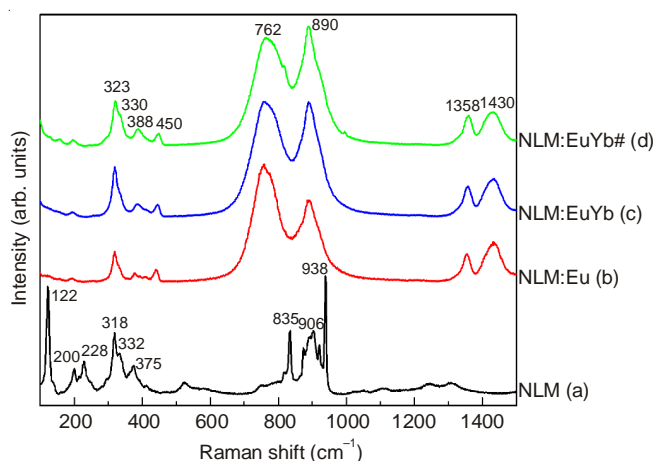


Fig. 5. Raman spectra of the synthesized (a)  $\text{NaLa}(\text{MoO}_4)_2(\text{NLM})$ , (b)  $\text{NaLa}_{0.5}(\text{MoO}_4)_2:\text{Eu}_{0.05}\text{Yb}_{0.45}(\text{NLM}:\text{Eu})$ , (c)  $\text{NaLa}_{0.7}(\text{MoO}_4)_2:\text{Eu}_{0.1}\text{Yb}_{0.2}(\text{NLM}:\text{EuYb})$  and (d)  $\text{NaLa}_{0.5}(\text{MoO}_4)_2:\text{Eu}_{0.05}\text{Yb}_{0.45}(\text{NLM}:\text{EuYb}\#)$  particles excited by the 514.5 nm line of an Ar ion laser at 0.5 mW

$\text{Eu}_{0.1}\text{Yb}_{0.2}(\text{NLM}:\text{EuYb})$  and (d)  $\text{NaLa}_{0.5}(\text{MoO}_4)_2:\text{Eu}_{0.05}\text{Yb}_{0.45}(\text{NLM}:\text{EuYb}\#)$  particles excited by the 514.5 nm line of an Ar ion laser at 0.5 mW. The internal modes for the (a)  $\text{NaLa}(\text{MoO}_4)_2(\text{NLM})$  particles were detected at 220, 228, 318, 332, 375, 835, 906 and 938  $\text{cm}^{-1}$ , respectively. The well-resolved sharp peaks for the  $\text{NaLa}(\text{MoO}_4)_2(\text{NLM})$  particles indicate a high crystallinity state of the synthesized particles. The internal vibration mode frequencies are dependent on the lattice parameters and the degree of the partially covalent bond between the cation and molecular ionic group  $[\text{MoO}_4]^{2-}$ . The Raman spectra of  $\text{NaLa}_{0.8}(\text{MoO}_4)_2:\text{Eu}_{0.2}$ ,  $\text{NaLa}_{0.7}(\text{MoO}_4)_2:\text{Eu}_{0.1}\text{Yb}_{0.2}$  and  $\text{NaLa}_{0.5}(\text{MoO}_4)_2:\text{Eu}_{0.05}\text{Yb}_{0.45}$  particles indicated the domination of strong peaks at higher frequencies (762, 890, 1358 and 1430  $\text{cm}^{-1}$ ) and weak peaks at lower frequencies (323, 388 and 450  $\text{cm}^{-1}$ ). The doped particles prove that the doping ions can influence the structure of the host materials. The combination of a heavy metal cation and the inter-ionic distance for  $\text{Eu}^{3+}$  and  $\text{Yb}^{3+}$  substitutions in  $\text{La}^{3+}$  sites in the lattice result in a high probability of UC and phonon-splitting relaxation in  $\text{NaLa}_{1-x}(\text{MoO}_4)_2:\text{Eu}^{3+}/\text{Yb}^{3+}$  crystals. It is assumed that these very strong and strange effects are generated by the disorder of the  $[\text{MoO}_4]^{2-}$  groups with the incorporation of the  $\text{Eu}^{3+}$  and  $\text{Yb}^{3+}$  elements into the crystal lattice or by a new phase formation<sup>15</sup>.

## Conclusion

$\text{NaLa}_{1-x}(\text{MoO}_4)_2:\text{Eu}^{3+}/\text{Yb}^{3+}$  phosphors with doping concentrations of  $\text{Eu}^{3+}$  and  $\text{Yb}^{3+}$  ( $x = \text{Eu}^{3+} + \text{Yb}^{3+}$ ,  $\text{Er}^{3+} = 0.05$ ,

0.1, 0.2 and  $\text{Yb}^{3+} = 0.2, 0.45$ ) were successfully synthesized via the microwave-modified sol-gel route showing a fine and homogeneous morphology with particle sizes of 5-10  $\mu\text{m}$ . The upconversion intensities of  $\text{NaLa}_{0.7}(\text{MoO}_4)_2:\text{Eu}_{0.1}\text{Yb}_{0.2}$  and  $\text{NaLa}_{0.5}(\text{MoO}_4)_2:\text{Eu}_{0.05}\text{Yb}_{0.45}$  particles exhibited a strong 525 nm emission band in the green region, a weak 475 nm emission band in the blue region and a very weak 655 nm emission band in the red region. The strong 525 nm emission in the green region corresponds to the  ${}^7\text{F}_1 \rightarrow {}^5\text{D}_1$  transition and the weak 475 nm emission in the blue region corresponds to the  ${}^7\text{F}_0 \rightarrow {}^5\text{D}_2$  transition, while the very weak emission 655 nm band in the red region corresponds to the  ${}^5\text{D}_0 \rightarrow {}^7\text{F}_3$  transition. The upconversion intensity of  $\text{NaLa}_{0.5}(\text{MoO}_4)_2:\text{Eu}_{0.05}\text{Yb}_{0.45}$  is much higher than that of  $\text{NaLa}_{0.7}(\text{MoO}_4)_2:\text{Eu}_{0.1}\text{Yb}_{0.2}$  particles. The Raman spectra of  $\text{NaLa}_{0.8}(\text{MoO}_4)_2:\text{Eu}_{0.2}$ ,  $\text{NaLa}_{0.7}(\text{MoO}_4)_2:\text{Eu}_{0.1}\text{Yb}_{0.2}$  and  $\text{NaLa}_{0.5}(\text{MoO}_4)_2:\text{Eu}_{0.05}\text{Yb}_{0.45}$  particles indicated the domination of strong peaks at higher frequencies (762, 890, 1358 and 1430  $\text{cm}^{-1}$ ) and weak peaks at lower frequencies (323, 388 and 450  $\text{cm}^{-1}$ ).

## ACKNOWLEDGEMENTS

This study was supported by the Basic Science Research Program through the National Research Foundation of Korea (NRF) funded by Ministry of Science, ICT & Future Planning (2014-046024).

## REFERENCES

1. M. Lin, Y. Zhao, S.Q. Wang, M. Liu, Z.F. Duan, Y.M. Chen, F. Li, F. Xu and T.J. Lu, *Biotechnol. Adv.*, **30**, 1551 (2012).
2. M. Wang, G. Abbineni, A. Clevenger, C. Mao and S. Xu, *Nanomedicine*, **7**, 710 (2011).
3. A. Shalav, B.S. Richards and M.A. Green, *Sol. Energy Mater. Sol. Cells*, **91**, 829 (2007).
4. C. Guo, H.K. Yang and J.H. Jeong, *J. Lumin.*, **130**, 1390 (2010).
5. J. Liao, D. Zhou, B. Yang, R. Liu, Q. Zhang and Q. Zhou, *J. Lumin.*, **134**, 533 (2013).
6. J. Sun, J. Xian and H. Du, *J. Phys. Chem. Solids*, **72**, 207 (2011).
7. T. Li, C. Guo, Y. Wu, L. Li and J.H. Jeong, *J. Alloys Comp.*, **540**, 107 (2012).
8. M. Nazarov and D.Y. Noh, *J. Rare Earths*, **28**, 1 (2010).
9. J. Sun, W. Zhang, W. Zhang and H. Du, *Mater. Res. Bull.*, **47**, 786 (2012).
10. S. Das, A.K. Mukhopadhyay, S. Datta and D. Basu, *Bull. Mater. Sci.*, **32**, 1 (2009).
11. T. Thongtem, A. Phuruangrat and S. Thongtem, *J. Nanopart. Res.*, **12**, 2287 (2010).
12. J. Zhang, X. Wang, X. Zhang, X. Zhao, X. Liu and L. Peng, *Inorg. Chem. Commun.*, **14**, 1723 (2011).
13. J. Sun, J. Xian, X. Zhang and H. Du, *J. Rare Earths*, **29**, 32 (2011).
14. Q. Sun, X. Chen, Z. Liu, F. Wang, Z. Jiang and C. Wang, *J. Alloys Comp.*, **509**, 5336 (2012).
15. C.S. Lim, *Mater. Res. Bull.*, **48**, 3805 (2013).